https://doi.org/10.5194/acp-2019-519
Preprint. Discussion started: 25 July 2019


Atmospheric Chemistry and Physics Discussions

# Hygroscopic properties and CCN activity of atmospheric aerosols under the influences of Asian continental outflow and new particle formation at a coastal site in East Asia

Hing Cho Cheung[1,2], Charles C.-K. Chou[3*], Celine S. L. Lee[3], Wei-Chen Kuo[3], Shuenn-Chin Chang[4,5]

[1]School of Atmospheric Sciences, and Guangdong Province Key Laboratory for Climate Change and Natural Disaster Studies, Sun Yat-sen University, Guangzhou 510275, China

[2]Southern Laboratory of Ocean Science and Engineering (Guangdong, Zhuhai), 519082, China

[3]Research Center for Environmental Changes, Academia Sinica, Taipei 11529, Taiwan

[4]Environmental Protection Administration, Taipei 10042, Taiwan

[5]School of Public Health, National Defense Medical Center, Taipei 11490, Taiwan

**Corresponding author**:
Charles C.-K. Chou (ckchou@gate.sinica.edu.tw)

https://doi.org/10.5194/acp-2019-519
Preprint. Discussion started: 25 July 2019


Atmospheric Chemistry and Physics Discussions

**Abstract**

The chemical composition of fine particulate matters ($PM_{2.5}$), the size distribution and number concentration of aerosol particles ($N_{CN}$) and the number concentration of cloud condensation nuclei ($N_{CCN}$) were measured at the northern tip of Taiwan Island during a campaign from April 2017 to March 2018. The parameters of aerosol hygroscopicity (i.e. activation ratio, activation diameter and kappa) were retrieved from the measurements. Significant variations were found in the hygroscopicity of aerosols, which were suggested be subject to various pollution sources, including aged air pollutants originating in the eastern/northern China and transported on the Asian continental outflows, fresh particles emitted from local sources and distributed by land-sea breeze circulations as well as produced by new particle formation (NPF) processes. Cluster analysis was applied to the backward trajectories of air masses to investigate their respective source regions. The results showed that the aerosols associated with Asian continental outflows were characterized with higher kappa values, whereas higher $N_{CCN}$ and $N_{CN}$ with lower kappa values were found for aerosols in local air masses. The distinct features in hygroscopicity were consistent with the characteristics in the chemical composition of $PM_{2.5}$. Moreover, this study revealed that the nucleation mode particles from NPF could have participated in the enhancement of CCN activity, most likely by coagulating with sub-CCN particles, although the freshly produced particles were not favored for CCN activation due to their smaller sizes. Thus, the results of this study suggested that the NPF coupling with coagulation processes can significantly increase the $N_{CCN}$ in atmosphere.

**Keywords**: Cloud condensation nuclei, Asian continental outflows, aerosol hygroscopicity, kappa of aerosols

https://doi.org/10.5194/acp-2019-519
Preprint. Discussion started: 25 July 2019


Atmospheric Chemistry and Physics Discussions

## 1. Introduction

Aerosols suspended in the atmosphere allow condensation of water vapor under certain super-saturation conditions and subsequently evolve into cloud droplets. Activation of cloud condensation nuclei (CCN) depends on the size and chemical composition of aerosol particles, as well as on the meteorological conditions (i.e. water vapor supersaturation (SS), and uplift force for air parcels) (Seinfeld and Pandis 1998). Among the chemical and physical properties of aerosols, hygroscopicity plays critical roles in the complex aerosol-cloud interactions (McFiggans et al., 2006; Lee et al., 2010). Atmospheric aerosols are a mixture of different chemical species rather than a single compound and exist in various size ranges and mixing states. A single parameter called kappa (κ) has been developed to evaluate hygroscopicity of aerosols, which represents a scaled volume fraction of soluble materials in particles and provides a theoretical framework to derive bulk hygroscopicity for aerosols with internal mixtures (Petters and Kreidenweis, 2007). However, while the hygroscopicity and CCN activity of a single component can be characterized in laboratories, the properties of their mixture in ambient air are difficult to estimate owing to the complexity in physiochemical characteristics of aerosols. Thus, field investigations have been conducted to study aerosol hygroscopicity and CCN activity in various environmental settings including rural, urban, forest and marine boundary layer (Ehn et al., 2007; Massling., 2007; Gunthe et al., 2009; Wu et al., 2016; Schmale et al., 2017; Park et al., 2018). Furthermore, in-situ measurements of physicochemical properties of aerosols and CCN in critical geographical areas in climate system could provide a means of constraining representation of relevant schemes in global climate models (Khairoutdinov and Randall, 2001; Betancourt and Nenes, 2014; Seinfeld et al., 2016).

Due to the rapid industrialization and economic development in the East Asia (EA) during the past few decades, the EA has become one of the most polluted regions in the world where significant amount of particulate matters (PM) and their precursors were emitted (Streets et al., 2003; Dentener et al., 2006; Zhang et al., 2009). Taiwan is located in the downwind area of the EA continental outflows, and thereby is influenced by the pollution outbreaks during the winter monsoon seasons. Besides, the air quality in Taiwan is also known to be affected by the photochemical production of secondary aerosols. The geographical location thus provides a strategic platform to investigate the CCN activation of aerosols influenced by a complex mixture of pollutants (Chou et al., 2005, 2017; Chang et al., 2010; Cheung et al., 2013, 2016; Li et al., 2016; Lee et al., 2019). Cheung et al. (2013) reported that new particle formation

https://doi.org/10.5194/acp-2019-519
Preprint. Discussion started: 25 July 2019


Atmospheric Chemistry and Physics Discussions

(NPF) events occurred frequently during summertime in Taiwan, where the number concentration of nucleation mode particles formed from photochemical reactions was nearly ten-fold of that attributed to local primary pollution, indicating the critical impact of NPF on particle concentration. Previous studies suggested that the freshly formed particles could further grow into larger particles by up-taking condensable vapors (i.e. organic and sulfuric vapors) and increased CCN concentration (Merikanto et al., 2009; Pierce et al., 2012); however, the detailed processes were not clear yet. To date, most of the studies upon CCN and its interaction with NPF have been conducted in Europe and North America, whereas only a few short-term intensive studies in East Asia were available despite the frequent NPF observed in this region (Yue et al., 2011; Leng et al., 2014; Ma et al., 2016). In order to investigate the hygroscopicity and CCN activity of the aerosols with a complex pollution sources and aging processes, a one-year observation study on characteristics of aerosols and CCN was conducted in the northern Taiwan. The aim of this study was to characterize the variations in aerosol hygroscopicity and CCN activity under the influences of continental outflows and new particle formation during different seasons.

## 2. Methodology

### *2.1 Observation site and instrumentation*

A field study was conducted at the Cape Fuguei Research Station (named CAFÉ, 25.30˚N, 121.54˚E, 10 m a.s.l.) located at the northern tip of Taiwan Island (see **Figure 1** for map) from 1 April 2017 to 31 March 2018. The air quality in northern Taiwan exhibited significant seasonal variations, depending on the origins of polluted air masses. The EA continental pollution outbreaks dominated during the seasons of winter monsoons, whereas local pollution associated with southerly flows affected the study site, particularly during summer (Chou et al., 2017). Therefore, this station provides an ideal platform for studies on the aerosol hygroscopicity and CCN activity under the influences of various pollution sources.

The aerosol sampling inlets were located at the rooftop of the station and ambient air was drawn into the instruments through conductive tubing. **Figure 2** illustrates the schematics of aerosol sampling. Two inlets were deployed for aerosol sampling and were equipped with diffusion dryers filled with silica gel to reduce RH. One of the inlets was for particle size distribution measurement (13-736 nm), which was carried out by a scanning mobility particle sizer (SMPS, TSI Inc.). The SMPS system consisted of an electrostatic classifier (TSI 3080) with long-differential mobility analyzer (TSI 3081) and a water-based condensation particle counter

https://doi.org/10.5194/acp-2019-519
Preprint. Discussion started: 25 July 2019


Atmospheric Chemistry and Physics Discussions

(WCPC, TSI 3786). The sheath and sample flow rates were 3 and 0.6 lpm, respectively, and the sample time interval was 5 minutes. The accuracy of particle sizing was checked using polystyrene latex spheres (PSLs). The nominal diameters of the PSLs were 97±3nm (Part#: 3100A, Thermo Scientific Inc.) and 240±5 nm (Part#: 3240A, Thermo Scientific Inc.). The averaged modes of the PSLs measured by the SMPS were found to be 100±2.1 and 232.9±0 nm, respectively, and the differences from the nominal diameters were within 3%. Multiple charge and diffusion loss corrections were applied to the particle size distribution data using the internal algorithm from the Aerosol Instrument Manager Software. Furthermore, diffusion loss in sampling tube was corrected according to the algorithm proposed by Holman (1972).

The sample air from another inlet split into two streams for the CCN ($N_{CCN}$) and total particle number concentrations ($N_{CN}$) measurements, respectively, which were used to calculate the CCN activation ratio (AR). The instruments for $N_{CCN}$ and $N_{CN}$ measurements were cloud condensation nuclei counter (CCNC-100, DMT Inc.) and butanol-based condensation particle counter (BCPC 3022, TSI Inc.). The calibrated super-saturation (SS) condition setting of the CCN counter was periodically changed from 0.15±0.01, 0.29±0.02, 0.53±0.03 to 0.86±0.05% with time interval of 21, 13, 13, and 13 minutes (a total of 1 hour for each cycle). The flow rates for the CCNC and BCPC instruments were 0.5 and 0.3 lpm, respectively, which were checked routinely during sampling periods by the DryCal flow calibrator (Defender 520, Mesa Labs Inc.). The SS calibration of CCN counter was conducted using ammonium sulfate particles at the start, middle and end of the campaign. It should be noted that the CCNC malfunctioned at the end of Aug 2017, and sampling was resumed from Oct 2017. Hence, data was not available during that period.

$PM_{2.5}$ samples were collected by two sequential sampling systems (PNS 18-3.1DM, Comde-Derenda GmbH) and both samplers were equipped with $PM_{2.5}$ sharp cut cyclone with 16.7 lpm sampling flow rate. One sampler was equipped with Teflon filters which were used for the analysis of soluble ions (i.e. $Na^+$, $NH_4^+$, $K^+$, $Mg^{2+}$, $Ca^{2+}$, $Cl^-$, $NO_3^-$, $SO_4^{2-}$) using ion chromatograph (IC). Another sampler was equipped with quartz filters which were used for analysis of carbonaceous components (i.e. organic carbon, OC, and elemental carbon, EC) using a DRI-20001A carbonaceous aerosol analyzer with IMPROVE-A protocol (Chow et al., 2007). Details of the in-lab analysis are as described previously (Salvador and Chou, 2014). The sampling duration of each sample set was from 08:00 to 08:00LT (24h), and in total 282 samples were collected during the entire sampling period. Moreover, to assist the data

https://doi.org/10.5194/acp-2019-519
Preprint. Discussion started: 25 July 2019


Atmospheric Chemistry and Physics Discussions

interpretation, the hourly average mass concentration of $PM_{2.5}$, the mixing ratio of trace gases (i.e. CO, $O_3$, $SO_2$ and $NO_2$) and the meteorological parameters (i.e. wind direction/speed) reported from the air quality station of Taiwan EPA that collocated with the CAFÉ station were analyzed in this study.

2.2 *Data processing and analysis for aerosol hygroscopicity*

Firstly, the $N_{CCN}$ and $N_{CN}$ data were synchronized into 5 mins averaged data which matched the time interval for PSD data measured by SMPS. The CCN activation ratio (AR), i.e. the ratio of $N_{CCN}$ to $N_{CN}$, was calculated for a given SS condition. Given the assumption that the particles are homogeneously internally mixed and larger particles are activated first. Also, the number concentration of particles out of the measured particle size range is assumed negligible. The minimum diameter ($D_{ss}$) required for the CCN activation with the AR value at a given SS condition was calculated according to equation (1) (Hung et al., 2014).

$$AR = \frac{N_{CCN}}{N_{CN}} = \frac{\int_{D_{SS}}^{D_f} n(D)dlnD}{\int_{D_i}^{D_f} n(D)dlnD} \quad (1)$$

where n(D) is the number concentration while $D_i$ and $D_f$ are the first and final bin sizes based on SMPS data, respectively.

The hygroscopicity parameter (κ) was then calculated as the followings :

$$\kappa = \frac{4A^3}{27D_d^3 ln^2 S_c} \quad (2)$$

$$A = \frac{4\sigma_{S/W} M_W}{RT\rho_W} \quad (3)$$

where $S_c$ is the water saturation (= SS + 1), $D_d$ is the dry particle diameter and equivalent to $D_{ss}$ calculated by equation (1), $\sigma_{S/W}$ is the solution surface tension (0.072 J $m^{-2}$), $\rho_W$ is the water density (997 kg $m^{-3}$), $M_W$ is the molecular weight of water (0.018 kg $mole^{-1}$), R is the universal gas constant (8.314 J $K^{-1}$ $mole^{-1}$) and T is ambient temperature.

The kappa value is used to describe the hygroscopicity of the aerosols; for example, ammonium nitrate and ammonium sulfate have kappa values of 0.67 and 0.61, respectively, whereas it is ~

https://doi.org/10.5194/acp-2019-519
Preprint. Discussion started: 25 July 2019


Atmospheric Chemistry and Physics Discussions

0.1-0.2 for organic species (Petters and Kreidenweis, 2007). To remove the outliers in kappa data, we defined an outlier by values larger or smaller than 1.5 inter-quarter range (IQR) as following:

$$Q1 - 1.5\,IQR \; or \; Q3 + 1.5\,IQR \quad (4)$$

where Q1 and Q3 are first and third quarterly of kappa data, and IQR is Q3 minus Q1.

*2.3 Back-trajectories cluster analysis*

Five-day backward trajectories of air masses were calculated in every 4 hours using the Hybrid Single-Particle Lagrangian Integrated Trajectory (HYSPLIT) model of NOAA (National Oceanic and Atmospheric Administration) for the entire sampling period (Stein et al., 2015). The meteorological data used in the model were the 6-hourly Global Data Assimilation System (GDAS) archived data with a resolution of 0.5 degree in longitude and latitude. The end-point of the trajectories was 200 m above ground level at the CAFÉ station. Cluster analysis was then used to group trajectories into 5 clusters (see **Figure 3**). The air masses of Clusters 1, 2 and 4 were associated with Asian continental outflows induced by the high pressure system during autumn to spring seasons. The air-mass members of both Clusters 1 and 2 were originating in the inlands of the Asian continent, but the movement of Cluster 2 air masses was faster and from higher altitudes. Air masses in Cluster 4 were also induced by high pressure system but were moving slowly toward the Pacific Ocean and along marine boundary before reaching CAFÉ station. In contrast, Clusters 3 and 5 include air masses originating in the Pacific areas and passing through Taiwan Island during warm seasons. The occurrence frequency of each cluster is listed in **Table 1**. The implications of origins and trajectories of air masses for CCN activation will be discussed in details in Section 3.2.

## 3. Results and discussion

In the followings we first present the overall statistics of aerosol hygroscopicity and CCN activity, and the seasonal and diurnal variations. Then, the features in aerosol hygroscopicity for respective air mass clusters are depicted. Finally, the implications of NPF for CCN activity will be discussed.

*3.1. Overall statistics for seasonal and diurnal variations of aerosol hygroscopicity*

Statistics of the number concentration of cloud condensation nuclei ($N_{CCN}$) and total particles

https://doi.org/10.5194/acp-2019-519
Preprint. Discussion started: 25 July 2019


Atmospheric Chemistry and Physics Discussions

($N_{CN}$) as well as of the activation ratio (AR), activation diameter ($D_{SS}$) and kappa (κ) values under four SS conditions are summarized in **Table 2**. The median $N_{CCN}$ ranged from 820 to1880 $cm^{-3}$ for SS = 0.15 – 0.86 %. The median κ values calculated for the sampling period ranged from 0.17 to 0.62 (SS = 0.15 – 0.86 %), which exhibited larger variations than that reported from coastal sites in Hong Kong (κ: 0.28 – 0.39 for SS: 0.15 – 0.70%, Meng et al. 2014) and in Noto Peninsula, Japan (κ: 0.19 – 0.37 for SS: 0.13 – 0.81%, Iwamoto et al. 2016). Schmale et al. (2018) summarized the results of CCN measurements reported from 12 sites on 3 continents. The standardized κ values at SS of 0.5 % were found to be 0.48, 0.41, 0.55, and 0.30 for rural background, alpine, coastal background, and urban environmental settings, respectively. The estimated κ value at SS of 0.5 % was 0.31 for this study, which was significantly lower than that for coastal background and was more similar to that of urban aerosols. This is likely because the aerosol composition at CAFÉ station were frequently influenced by urban air pollution, as indicated in previous studies (Chou et al., 2008, 2010, 2017).

It is noteworthy that both the κ and $D_{SS}$ decrease with the SS, which implies some small and less hygroscopic particles getting activated at higher SS. Previous studies on size-resolved chemical composition of $PM_{2.5}$ at northern Taiwan reported that the size distribution of aliphatic carbons peaked at 0.12-0.15 μm and 0.62-0.87 μm while that for carbonyl carbons peaked only at 0.6-0.64 μm (Chou et al., 2005). Cheung et al. (2016) showed that the ultra-fine particles (i.e. d < 100 nm) collected from Taipei City, an urban site in northern Taiwan, consisted mostly of organic matters. Moreover, Salvador et al. (2016) revealed that low-molecular-weight organic acids were abundant in the submicron aerosols in Taipei, Taiwan. In this context, the low hygroscopicity of small aerosols found in this study was consistent with the results of investigations upon aerosol chemical composition.

**Figure 4** illustrates the monthly median with the first / third quartiles of $N_{CCN}$, kappa and $D_{SS}$ under SS of 0.29% and $N_{CN}$ for the entire campaign period. Distinct seasonal variations were observed in the measurements. Elevated levels of $N_{CN}$ and $N_{CCN}$ were observed in April (spring time) and July 2017 (summer time) (median 1540-1700 $cm^{-3}$). During spring and summer of 2017, NPF events were observed frequently which induced an elevated $N_{CN}$ (maximum median: 5650 $cm^{-3}$ in July 2017). The consistency in $N_{CN}$ and $N_{CCN}$ suggested that the particles generated by NPF processes could have contributed significantly to the increases in $N_{CCN}$. On

https://doi.org/10.5194/acp-2019-519
Preprint. Discussion started: 25 July 2019


Atmospheric Chemistry and Physics Discussions

the other hand, according to the kappa values, more hygroscopic particles were observed in June and October 2017. The variations of κ values could be under the influences of several mechanisms. The EA continental outflows affected the study site frequently in the seasons of EA winter monsoons, during which more inorganic aerosols could have been transported to the study site. Strong surface winds of winter monsoons could have also increased the production of sea salt particles around the coastal site and, thereby, resulted in increases in the kappa values. In addition, up-taking hygroscopic species during particle growth and coagulation processes may influence the hygroscopicity of aerosols, which will be discussed in further details later on.

**Figure 5** depicts the variations in daily chemical composition of $PM_{2.5,}$ where a higher fraction of inorganic pollutants was found during Apr. – May 2017 and Feb. – Mar. 2018, whereas sea-salt elevated during Oct. 2017 – Jan. 2018. The seasonality of aerosol composition was consistent with the long-term records of aerosol observation at this site (Chou et al., 2017). Petters and Kreidenweis (2007) have estimated CCN-derived κ values for inorganic and organic species, which showed that significantly higher κ values were found for major inorganics species in aerosols, such as ammonium sulfate, ammonium nitrate, sodium chloride (kappa: 0.61-1.28), while κ values for organic species were usually lower than 0.2. Thus, relatively lower kappa values observed during Jul. – Aug. 2017 were consistent to the $PM_{2.5}$ chemical composition data in which a higher mass fraction of organic carbon was found.

3.2 *Implications of different types of air masses*

The air masses reaching this study site are known to be associated with the Asian continental outflows and/or with local pollution in northern Taiwan (Cheung et al., 2016). Since CO has longer atmospheric lifetime than $NO_2$, a higher $\Delta CO/\Delta NO_2$ can be used to indicate influences of aged regional air pollutants. The averaged median $\Delta CO/\Delta NO_2$ ratios for the 5 trajectory clusters were 76, 75, 32, 60 and 33, respectively. A higher $\Delta CO/\Delta NO_2$ ratio was found in Clusters 1, 2 and 4, whereas $\Delta CO/\Delta NO_2$ of Cluster 4 was found slightly lower than that of Cluster 1 and 2. This was attributed to the differences in air mass history; the air masses of both Clusters 1 and 2 were originating in the inland areas of the Asian Continent, whereas the air masses of Cluster 4 passed through the south of Korea and Japan and came from the east of CAFÉ station and, thereby, was occasionally impacted by some fresh emissions. The mixing ratio of $O_3$, a typical secondary pollutant, provided further information about the sources of air plumes. The results showed that higher $O_3$ levels (43-46 ppb) were found in continental

https://doi.org/10.5194/acp-2019-519
Preprint. Discussion started: 25 July 2019


Atmospheric Chemistry and Physics Discussions

outflows (i.e. Cluster 1, 2 and 4) as compared to those of marine air masses (i.e. 26-28 ppb for Cluster 3 and 5).

Furthermore, higher κ values were found for CCN transported with the continental outflows, which ranged from 0.19 to 0.69 for SS of 0.15-0.86 %. On the contrary, lower κ values (0.14 - 0.56) were found for the CCN in air mass of Clusters 3 and 5, which originated in the remote Pacific region and passed through Taiwan Island during summertime. This result was reasonable since aged polluted air masses contained more inorganic species (with higher κ values), while the organic species (with lower κ values) contributed a higher fraction to the aerosol mass loading in urban areas of Taiwan (Chou et al., 2010, 2017). On the other hand, higher $N_{CCN}$ and $N_{CN}$ were found in Clusters 3 and 5 compared to that in Clusters 1 and 2 (see **Table 3**). This could be due to the substantial production of new particles during warmer seasons (Cheung et al., 2013, 2016).

### 3.3 *Implications of New Particle Formation*

As described in **Section 3.1**, large variations in $N_{CCN}$ and kappa values were found in summer during which NPF events occurred frequently. A NPF event is defined as the increase of the number concentration of nucleation mode particles, and those particles are growing into Aitken and/or accumulation mode size range ($\geqslant$ 25nm) and last for a few hours until they disappear into the atmosphere by condensation/coagulation sinks (Dal Maso et al., 2005). In total 53 NPF events were observed during the entire study period and among which 31 were observed in warm months (from June to September 2017), representing an occurrence frequency of 58.5%. Investigations reported that NPF occurred more frequently during summer (34.6 - 42.8%) and occasionally during spring (11.5%) in urban areas of northern Taiwan (Cheung et al., 2013, 2016). **Figure 6** illustrates the median particle size distribution for NPF and non-NPF days as well as the quartiles. The particle number concentration for NPF events was significantly higher than that for non-NPF case. In addition, large variations were associated with the particle size below 100 nm in NPF events, suggesting that a large amount of ultra-fine particles formed.

In **Figure 7**, diurnal variations in particle size distribution for NPF and non-NPF cases are presented along with the aerosol hygroscopic parameters $D_{SS}$, κ and AR at SS = 0.29 %. In the plot of particle size distribution for NPF events, a banana feature (growth of particle diameter indicated by the geometric mean diameter, GMD) is obviously illustrated, which is typical for

https://doi.org/10.5194/acp-2019-519
Preprint. Discussion started: 25 July 2019


Atmospheric Chemistry and Physics Discussions

NPF process (Dal Maso et al., 2005; Cheung et al., 2011), while relatively stable particle size distribution exhibites for non-NPF periods with the particles of 50-60 nm dominate throughout a day.

On NPF days, a nucleation burst as indicated by a surge in nucleation mode particles ($N_{30}$, number concentration of particle size ≤ 30 nm) from 06:00 to 10:00 LT was observed (as shown in **Figure 7**). Note that the number concentration of Aitken mode particles (indicated by $N_{30\text{-}100}$, for particle size between 30 to 100 nm) increased consistently, implying coagulation was active during the period. $N_{CCN}$ started to increase significantly around 07:00 LT. It was found that the increasing rate of $N_{CN}$ was higher than that of $N_{CCN}$, which in turn resulted in the decreases in AR. The increases in $N_{CCN}$ were attributed to coagulation processes. **Figure 8** illustrates schematically the CCN enhancement by coagulation processes at the initial stage of a NPF event. Once the NPF process starts, the freshly formed nucleation mode particles could get coagulated with the pre-existing particles, with either CCN or sub-CCN sizes. The preexisting sub-CCN particles coagulate with the newly formed particles and, as a result, grow rapidly into CCN and thereby increase the $N_{CCN}$. On the other hand, the new particles could also coagulate with the preexisting CCN, which should not increase the $N_{CCN}$ but will result in an increase in the size of CCN. The observation of this study (see **Figure 7**) showed that $D_{SS}$ slightly increased from about 80 nm at 04:00 LT to 87nm at 08:00 LT, suggesting that preexisting CCN particles were still predominant in this stage despite the production of "new CCN" has resulted in the increases in $N_{CCN}$. Several observational studies reported that enhancement of CCN number concentrations were associated with NPF process (Sihto et al., 2011; Yue et al., 2011; Leng et al., 2014; Wu et al., 2015). However, the time for the newly formed nano-particles growing to CCN sizes ranges from a few hours to more than a day (Keriminen et al., 2018). Hence the enhancement of CCN at the initial stage of a NPF event as observed in this study cannot be explained by the growth of new particles, and was most likely due to coagulation among the newly formed particles and pre-existing particles.

At a later stage, because the coagulation sink exceeds the production rate of new particles, the $N_{CN}$ turn to decrease, whereas the $N_{CCN}$ keeps the increasing trend for the production of new CCN by coagulation among particles. As a result of increases in $N_{CCN}$ and decreases in $N_{CN}$, a significant increase in AR is expected. This has been observed in this study. **Figure 7** illustrates that the AR on NPF days increased rapidly since 10:00 LT, in phase with the drastic decreases in the number density of $N_{30}$ and $N_{30\text{-}100}$. Agreeing with the earlier stage, the increased $N_{CCN}$

https://doi.org/10.5194/acp-2019-519
Preprint. Discussion started: 25 July 2019


Atmospheric Chemistry and Physics Discussions

was suggested a result of the coagulation between nucleation mode particles and the Aiken mode particles in sub-CCN size range, which thus grew into CCN size range. However, as more and more "new CCN" formed along with the NPF processes, which would become majority in the CCN population and thereby shift the size distribution of CCN to the left (as shown in **Figure 8**). This inference was evidenced by the observation in this study, where the decrease in $D_{SS}$ from 87 nm at 08:00 LT to 74 nm at 15:00 LT was found. It should be noted that the transport of external CCN during the particle growth process could also increase the CCN concentration; however, this influence should be minor because it cannot explain the simultaneous changes in $N_{CN}$ and AR.

It was found that the kappa values exhibited a decreasing trend in the early stage of NPF and turned to an increase from 0.26 to 0.41 during the later stage. Similar increase of κ values during the particle growth period was also observed in a suburban region of northern China (Li et al., 2017). The κ values reached ~ 0.4 after the growth process, which was likely a result of a mixture of hygroscopic species like ammonium sulfate (κ = 0.61) and organic matters (κ = 0.1 – 0.2). This is evidenced by the measurement of chemical composition as shown in **Figure 5**, where the $PM_{2.5}$ was composed mostly of sulfate and organic carbon, particularly during the warm months with frequent NPF events. Note that the chemical composition of ultrafine particles at urban Taipei was dominated by organic carbon (Cheung et al., 2016), which generally has lower κ values. Therefore, coagulation of the ultrafine organic particles and the larger preexisting CCN particles may have reduced the kappa values of the CCN during the initial stage of NPF.

In contrast, the increases in kappa during the later NPF course suggested that the "new CCN" were dominated by hygroscopic species. The field studies at North China Plain found two types of NPF events (Yue et al., 2010, Ma et al. 2016), including sulfur-rich NPF, i.e., condensation and neutralization of sulfuric acid contributed most to the growth of the new particles with high particle hygroscopicity, and sulfur-poor NPF, i.e., condensation of organic compounds had a higher contribution to the growth with a lower particle hygroscopicity. Our results showed that the NPF events in northern Taiwan were characterized by elevated levels in both sulfur and organic matters (as shown in **Figure 5**). In particular, the submicron particles in northern Taiwan were found enriched in sulfate (Cheung et al., 2016) and organic acids (Salvador et al., 2016). Thus it was inferred that the preexisting sub-CCN particles were more hygroscopic, which resulted in the increases in kappa when they evolved into CCN through coagulation with

https://doi.org/10.5194/acp-2019-519
Preprint. Discussion started: 25 July 2019


Atmospheric Chemistry and Physics Discussions

ultrafine particles. The growth of sub-CCN particles at the study site could also be due to condensation of organic compounds. However, as illustrated in **Figure 8**, the composition of "new CCN" are dominated by the preexisting sub-CCN particles and thereby characterized with high kappa values. In this context, the increases in $N_{CCN}$ during the NPF events were unlikely contributed from the condensation growth of newly formed particles.

The result of this study is similar to the previous studies which indicated that an enhancement of CCN number was associated with the NPF process. The increase of CCN was observed in a few hours (Yue et al., 2011; Wu et al., 2015; Leng et al., 2014) to a few days after the start of the NPF (Sihto et al., 2011). However, distinct responses of the CCN activation diameter were observed. Sihto et al. (2011) indicated that $D_{SS}$ increased gradually with the increased of $N_{CCN}$, whereas Wu et al. (2015) showed a decrease in $D_{SS}$ once NPF process occurred and increased in the later stage. In the present work, $D_{SS}$ slightly increased once NPF started, and then decreased in later stage of the NPF event (see **Figure 7 and 8**). The discrepancy observed in respective studies showed the complexity in the particle growth processes. Nevertheless, the results of this study suggest that NPF coupling with coagulation is an important process to enhance the number of CCN in the study region.

## 4. Conclusion

This study presented the observation of aerosol hygroscopicity parameters, including κ, CCN activation diameter ($D_{SS}$) and activation ratio (AR = $N_{CCN}/N_{CN}$), at a coastal research station (CAFÉ) in northern Taiwan during a 1-year campaign from April 2017 to March 2018. The parameters exhibited distinct seasonal variations. High levels of $N_{CN}$ and $N_{CCN}$ were consistently observed in spring and summer, whereas kappa elevated in autumn and exhibited minimal in summer. Measurements of the chemical composition of $PM_{2.5}$ and cluster analysis of the backward trajectories were deployed to elucidate the seasonality observed in the hygroscopicity of aerosols. The results of this study indicated that aerosols associated with Asian continental outflows contained more inorganic species and thereby were characterized with higher κ values, as comparing to those associated with local urban pollution which consisted substantially of organic matters.

The higher levels of $N_{CCN}$ and $N_{CN}$ found in spring and summer were attributed mainly to the NPF events occurred frequently during warm months. A two-stage hypothesis was proposed according to the results of this study for the implications of NPF for CCN activity. At the early

https://doi.org/10.5194/acp-2019-519
Preprint. Discussion started: 25 July 2019


Atmospheric Chemistry and Physics Discussions

stage of a NPF event, new particles formed and resulted in increases in $N_{30}$ and thereby $N_{CN}$, which was followed immediately by increases in the number density of Aiken mode particles ($N_{30-100}$). The new particles coagulated with preexisting sub-CCN particles, which thereby evolved into "new CCN" and resulted in the increases in $N_{CCN}$. The new particles coagulated also with the preexisting CCN and resulted in increases in $D_{ss}$ before the "new CCN" became predominant. At the later stage, along with the NPF and coagulation processes, $N_{30}$, $N_{30-100}$ and $N_{CN}$ decreased for the larger coagulation sink, whereas generation of "new CCN" continued and resulted in increases in $N_{CCN}$ and a significant enhancement in AR. The activation diameter got smaller ($D_{ss}$) as the "new CCN" overwhelming in the CCN population at this stage. Moreover, the investigation results showed that the kappa of CCN exhibited a decrease at the early stage and an increasing trend during the second stage. It was inferred accordingly that the newly formed particles were composed mostly of organic matters that "diluted" the hygroscopicity of preexisting CCN at the early stage, whereas the sub-CCN particles consisted of highly hygroscopic components dominated in the later stage of the event.

The seasonal characteristics of hygroscopicity and CCN activity under the influences of a complex mixture of pollutants from different regional and/or local pollution sources have been illustrated in this study, and the impacts of NPF was demonstrated. Nevertheless, the mixing state and chemical composition of the aerosols, in particular the organic content of the sea spray aerosols, would critically influence the aerosol hygroscopicity in coastal areas. Hence further investigations are necessitated to understand the atmospheric processing involved in the CCN activation which would in turn affect cloud formation and the regional climate.

**Author contributions**

HC Cheung performed the instrumentation and data analysis. CCK Chou initiated the research program, led the research team and was in charge of the chemical analysis. CSL Lee participated in science discussion. WC Kuo conducted data analysis for CCN. SC Chang was in charge of the operation of the air quality station of Taiwan EPA. HC Cheung prepared the manuscript with contributions from all co-authors.

**Acknowledgements**

The authors gratefully acknowledge the logistic support and access of station facility from the Research Center for Environmental Changes, Academia Sinica, and the financial supports from the Ministry of Science and Technology, Taiwan through grants 105-2111-M-001-004-MY3,

https://doi.org/10.5194/acp-2019-519
Preprint. Discussion started: 25 July 2019


Atmospheric Chemistry and Physics Discussions

105-2811-M-001-136, 106-2811-M-001-091, 106-3114-M-001-001-A and 107-2811-M-001-1563, as well as from the Academia Sinica through grant AS-KPQ-106- DDPP. We thank Tareq Hussein for providing us with the code of DO-FIT for particle size distribution fitting. We also thank the Center for Space and Remote Sensing Research (CSRSR), National Central University for providing and agreeing the use of satellite image of Taiwan.

## References

Chang, S.-C., Chou, C.C.-K., Chen, W.-N., and Lee, C.-T.: Asian dust and pollution transport – A comprehensive observation in the downwind Taiwan in 2006. Atmos. Res., 95, 19-31, https://doi.org/10.1016/j.atmosres.2009.07.012, 2010.

Cheung, H.C., Morawska, L., and Ristoviski, Z.D.: Observation of new particle formation in subtropical urban environment. Atmos. Chem. Phys., 11, 3823-3833, https://doi.org/10.5194/-11-3823-2011, 2011.

Cheung, H.C., Chou, C.C.-K., Huang, W.-R., and Tsai, C.-Y.: Characterization of ultrafine particle number concentration and new particle formation in an urban environment of Taipei, Taiwan. Atmos. Chem. Phys., 13, 8935-8946, https://doi.org/10.5194/-13-8935-2013, 2013.

Cheung, H.C., Chou, C.C.-K., Chen, M.-J., Huang, W.-R., Huang, S.-H., Tsai, C.-Y., and Lee, C.S.L.: Seasonal variations of ultra-fine and submicron aerosols in Taipei, Taiwan: implications for particle formation processes in a subtropical urban area. Atmos. Chem. Phys., 16, 1317-1330, https://doi.org/10.5194/-16-1317-2016, 2016.

Chou, C.C.-K., Huang, S.-H., Chen, T.-K., Lin, C.-Y., and Wang, L.-C.: Size-segregated characterization of atmospheric aerosols in Taipei during Asian outflow episodes. Atmos, Res., 75, 89-109, https://doi.org/10.1016/j.atmosres.2004.12.002, 2005.

Chou, C.C.-K., Lee, C.T., Yuan, C.S., Hsu, W.C., Lin, C.-Y., Hsu, S.-C., and Liu, S.C.: Implications of the chemical transformation of Asian outflow aerosols for the long-range transport of inorganic nitrogen species. Atmos. Environ., 42, 7508-7519, https://doi.org/10.1016/j.atmosenv.2008.05.049, 2008.

Chou, C.C.-K., Lee, C.T., Cheng, M.T., Yuan, C.S., Chen, S.J., Wu, Y.L., Hsu, W.C., Lung, S.C., Hsu, S.C., Lin, C.Y., and Liu, S.C.: Seasonal variation and spatial distribution of carbonaceous aerosol in Taiwan. Atmos. Chem. Phys., 10, 9563-9578, https://doi.org/10.5194/acp-10-9563-2010, 2010.

Chou, C.C.-K., Hsu, W.-C., Chang, S.-Y., Chen, W.-N., Chen, M.-J., Huang, W.-R., Huang, S.-

https://doi.org/10.5194/acp-2019-519
Preprint. Discussion started: 25 July 2019




H., Tsai, C.-Y., Chang, S.-C., Lee, C.-T., and Liu, S.-C.: Seasonality of the mass concentration and chemical composition of aerosols around an urbanized basin in East Asia. J. Geophys. Res., 122, 2026-2042, https://doi.org/10.1002/2016JD025728, 2017.

Chow, J.C., Watson, J.G., Chen, L., Chang, M., Robinson, N.F., Trimble, D., and Kohl, S.: The IMPROVE_A temperature protocol for thermal/optical carbon analysis: maintaining consistency with a long-term database. J. Air Waste Manage. Assoc., 57, 1014-1023, https://doi.org/10.3155/1047-3289.57.9.1014, 2007.

Dal Maso, M., Kulmala, M., Riipinen, I., Wagner, R., Hussein, T., Aalto, P.P., and Lehtinen, K.E.J.: Formation and growth of fresh atmospheric aerosols eight years of aerosol size distribution data from SMEAR II, Hyytiälä, Finland. Boreal Env. Res., 10, 323-336, 2005.

Dentener, F., Kinne, S., Bond, T., Boucher, O., Cofala, J., Generoso, S., Ginoux, P., Gong, S., Hoelzemann, J.J., Ito, A., Marelli, L., Penner, J.E., Putaud, J.-P., Textor, C., Schulz, M., van der Werf, G.R., and Wilson, J.: Emissions of primary aerosol and precursor gases in the years 2000 and 1750 prescribed data-sets for AeroCom. Atmos. Chem. Phys., 6, 4321-4344, https://doi.org/10.5194/acp-6-4321-2006, 2006.

Ehn, M. Petäjä, T. Aufmhoff, H., Aalto, P., Hämeri, K., Arnold, F., Laaksonen, A., and Kulmala, M.: Hygroscopic properties of ultrafine aerosol particles in the boreal forest: diurnal variation, solubility and the influence of sulfuric acid. Atmos. Chem. Phys., 7, 211-222, https://doi.org/10.5194/acp-7-211-2007, 2007.

Gunthe, S.S., King, S.M., Rose, D., Chen, Q., Roldin, P., Farmer, D.K., Jimenez, J.L., Artaxo, P., Andreae, M.O., Martin, S.T., and Poschl, U.: Cloud condensation nuclei in pristine tropical rainforest air of Amazonia: size-resolved measurements and modeling of atmospheric aerosol composition and CCN activity. Atmos. Chem. Phys., 9, 7551-7575, https://doi.org/10.5194/acp-9-7551-2009, 2009.

Holman, J.P.: Heat Transfer, McGraw-Hill, New York, 1972.

Hung, H.-M., Lu, W.-J., Chen, W.-N., Chang, C.-C., Chou, C.C.-K., and Lin, P.-H.: Enhancement of the hygroscopicity parameter kappa of rural aerosols in northern Taiwan by anthropogenic emissions. Atmos. Environ., 84, 78-87, https://doi.org/10.1016/j.atmosenv.2013.11.032, 2014.

Iwamoto, Y., Kinouchi, K., Watanabe, K., Yamazaki, N., and Matsuki, A.: Simultaneous Measurement of CCN Activity and Chemical Composition of Fine-Mode Aerosols at Noto Peninsula, Japan, in Autumn 2012. Aerosol Air Qual. Res., 16, 2107-2118, https://doi.org/10.4209/aaqr.2015.09.0545, 2016.



Kerminen, V.-M., Chen, X., Vakkari, V., Petaja, T., Kulmala, M., and Bianchi, F.: Atmospheric new particle formation and growth: review of field observations. Environ. Res. Lett., 13, 103003, https://doi.org/10.1088/1748-9326/aadf3c, 2018.

Khairoutdinov, M.F., and Randall, D.A.: A cloud-resolving model as a cloud parameterization in the NCAR Community Climate System Model: Preliminary results. Geophys. Res. Lett., 28, 3617-3620. https://doi.org/10.1029/2001GL013552, 2001.

Lee, C.S.L., Chou, C.C.-K., Cheung, H.C., Tsai, C.-Y., Huang, W.-R., Huang, S.-H., Chen, M.-J., Liao, H.-T., Wu, C.-F., Tsao, T.-M., Tsai, M.-J., and Su, T.-C.: Seasonal variation of chemical characteristics of fine particulate matter at a high-elevation subtropical forest in East Asia. Environ. Pollution, 246, 668-677, https://doi.org/10.1016/j.envpol.2018.11.033, 2019.

Lee, S.S., Donner, L.J. and Penner, J.E.: Thunderstorm and stratocumulus: how does their contrasting morphology affect their interactions with aerosols?. Atmos. Chem. Phys., 10, 6819-6837, https://doi.org/10.5194/acp-10-6819-2010, 2010.

Leng, C., Zhang, Q., Tao, J., Zhang, H., Zhang, D., Xu, C., Li, X., Kong, L., Cheng, T., Zhang, R., Yang, X., Chen, J., Qiao, L., Lou, S., Wang, H., and Chen, C.: Impacts of new particle formation on aerosol cloud condensation nuclei (CCN) activity in Shanghai: case study. Atmos. Chem. Phys., 14, 11353-11356, https://doi.org/10.5194/acp-14-11353-2014, 2014.

Li, T.-C., Yuan, C.-S., Huang, H.-C., Lee, C.-L., Wu, S.-P., and Tong, C.: Inter-comparison of seasonal variation, chemical characteristics, and source identification of atmospheric fine particles on both sides of the Taiwan Strait. Sci. Rep., 6, 22956, https://doi.org/10.1038/srep22956, 2016.

Li, Y., Zhang, F., Li, Z., Sun, L., Wang, Z., Li, P., Sun, Y., Ren, J., Wang, Y., Cribb, M., and Yuan, C.: Influences of aerosol physiochemical properties and new particle formation on CCN activity from observation at a suburban site of China. Atmos. Res., 188, 80-89, https://doi.org/10.1016/j.atmosres.2017.01.009, 2017.

Ma, N., Zhao, C., Tao, J., Wu, Z., Kecorius, S., Wang, Z., Größ, J., Liu, H., Bian, Y., Teich, M., Spindler, G., Müller, K., van Pinxteren, D., Herrmann, H., Hu, M., and Wiedensohler, A.: Variation of CCN activity during new particle formation events in the North China Plain. Atmos. Chem. Phys., 16, 8593-8607, https://doi.org/10.5194/acp-16-8593-2016, 2016.

Massling, A., Leinert, S., and Wiedensohler, A., Covert, D.: Hygroscopic growth of sub-micrometer and one-micrometer aerosol particles measured during ACE-Asia. Atmos. Chem. Phys., 7, 3249-3259, https://doi.org/10.5194/acp-7-3249-2007, 2007.

https://doi.org/10.5194/acp-2019-519
Preprint. Discussion started: 25 July 2019


Atmospheric Chemistry and Physics Discussions

McFiggans, G., Artaxo, P., Baltensperger, U., Coe, H., Facchini, M.C., Feingold, G., Fuzzi, S., Gysel, M., Laaksonen, A., Lohmann, U., Mentel, T.F., Murphy, D.M., O'Dowd, C.D., Snider, J.R. and Weingartner, E.: The effect of physical and chemical aerosol properties on warm cloud droplet activation. Atmos. Chem. Phys., 6, 2593-2649, https://doi.org/10.5194/acp-6-2593-2006, 2006.

Meng, J.M., Yueng, M.C., Li, Y.J., Lee, B.Y.L., and Chan, C.K.: Size-resolved cloud condensation nuclei (CCN) activity and closure analysis at the HKUST Supersite in Hong Kong. Atmos. Chem. Phys., 14, 10267-10282, https://doi.org/10.5194/acp-14-10267-2014, 2014.

Merikanto, J., Spracklen, D.V., Mann, G.W., Pickering, S.J., and Carslaw, K.S.: Impact of nucleation on global CCN. Atmos. Chem. Phys., 9, 8601-8616, https://doi.org/10.5194/acp-9-8601-2009, 2009.

Morales Betancourt, R., and Nenes, A.: Understanding the contributions of aerosol properties and parameterization discrepancies to droplet number variability in a global climate model. Atmos. Chem. Phys. 14, 4809-4826, https://doi.org/10.5194/acp-14-4809-2014, 2014.

Park, M., Yum, S.S., Kim, N., Cha, J.W., Shin, B., and Ryoo, S.-B.: Characterization of submicron aerosols and CCN over the Yellow Sea measured onboard the Gisang 1 research vessel using the positive matrix factorization analysis method. Atmos. Res., 214, 430-441, https://doi.org/10.1016/j.atmosres.2018.08.015, 2018.

Petters, M.D., and Kreidenweis, S.M.: A single parameter representation of hygroscopic growth and cloud condensation nucleus activity. Atmos. Chem. Phys., 7, 1961-1971, https://doi.org/10.5194/acp-7-1961-2007, 2007.

Pierce, J.R., Leaitch, W.R., Liggio, J., Westervelt, D.M., Wainwright, C.D., Abbatt, J.P.D., Ahlm, L., Al-Basheer, W., Cziczo, D.J., Hayden, K.L., Lee, A.K.Y., Li, S.-M., Russell, L.M., Sjostedt, S.J., Strawbridge, K.B., Travis, M., Vlasenko, A., Wentzell, J.J.B., Wiebe, H.A., Wong, J.P.S., and Macdonald, A.M.: Nucleation and condensational growth to CCN sizes during a sustained pristine biogenic SOA event in a forested mountain valley. Atmos. Chem. Phys., 12, 3147-3163, https://doi.org/10.5194/acp-12-3147-2012, 2012.

Salvador, C.M., and Chou, C.C.-K.: Analysis of semi-volatile materials (SVM) in fine particulate matter. Atmos. Environ., 95, 288-295, https://doi.org/10.1016/j.atmosenv.2014.06.046, 2014.

Salvador, C.M., Ho, T.-T., Chou, C. C.-K., Chen, M.-J., Huang, W.-R., and Huang, S.-H.: Characterization of the organic matter in submicron urban aerosols using a Thermo-

https://doi.org/10.5194/acp-2019-519
Preprint. Discussion started: 25 July 2019


Atmospheric Chemistry and Physics Discussions

Desorption Proton-Transfer-Reaction Time-of-Flight Mass Spectrometer (TD-PTR-TOF-MS). Atmos. Environ., 140, 565-575, https://10.1016/j.atmosenv.2016.06.029, 2016.

Schmale, J., Henning, S., Henzing, B., Keskinen, H., Sellegri, K., Ovadnevaite, J., Bougiatioti, A., Kalivitis, N., Stavroulas, I., Jefferson, A., Park, M., Schlag, P., Kristensson, A., Iwamoto, Y., Pringle, K., Reddington, C., Aalto, P., Aijälä, M., Baltensperger, U., Bialek, J., Birmili, W., Bukowiecki, N., Ehn, M., Fjæraa, A.M., Fiebig, M., Frank, G., Fröhlich, R., Frumau, A., Furuya, M., Hammer, E., Heikkinen, L., Herrmann, E., Holzinger, R., Hyono, H., Kanakidou, M., Kiendler-Scharr, A., Kinouchi, K., Kos, G., Kulmala, M., Mihalopoulos, N., Motos, G., Nenes, A., O'Dowd, C., Paramonov, M., Petäjä, T., Picard, D., Poulain, L., Prévôt, A.S.H., Slowik, J., Sonntag, A., Swietlicki, E., Svenningsson, B., Tsurumaru, H., Wiedensohler, A., Wittbom, C., Ogren, J.A., Matsuki, A., Yum, S.S., Myhre, C.L., Carslaw, K., Stratmann, F., and Gysel, M.: Collocated observations of cloud condensation nuclei, particle size distributions, and chemical composition. Sci. Data, 4, https://doi.org/10.1038/sdata.2017.3, 2017.

Schmale, J., Henning, S., Decesari, S., Henzing, B., Keskinen, H., Sellegri, K., Ovadnevaite, J., Pöhlker, M.L., Brito, J., Bougiatioti, A., Kristensson, A., Kalivitis, N., Stavroulas, I., Carbone, S., Jefferson, A., Park, M., Schlag, P., Iwamoto, Y., Aalto, P., Aijälä, M., Bukowiecki, N., Ehn, M., Frank, G., Frohlich, R., Frumau, A., Herrmann, E., Herrmann, H., Holzinger, R., Kos, G., Kulmala, M., Mihalopoulos, N., Nenes, A., O'Dowd, C., Petäjä, T., Picard, D., Pöhlker, C., Pöschl, U., Poulain, L., Prévôt, A.S.H., Swietlicki, E., Andreae, M.O., Artaxo, P., Wiedensohler, A., Ogren, J., Matsuki, A., Yum, S.S., Stratmann, F., Baltensperger, U., and Gysel, M.: Long-term cloud condensation nuclei number concentration, particle number size distribution and chemical composition measurements at regionally representative observatories. Atmos. Chem. Phys., 18, 2853-2881, https://doi.org/10.5194/acp-18-2853-2018, 2018.

Seinfeld, J.H., and Pandis, S.N.: Atmospheric Chemistry and Physics: from air pollution to climate change. John Wiley & Sons, New York, 1998.

Seinfeld, J.H., Bretherton, C., Carslaw, K.S., Coe, H., DeMott, P.J., Dunlea, E.J., Feingold, G., Ghan, S., Guenther, A.B., Kahn, R., Kraucunas, I., Kreidenweis, S.M., Molina, M.J., Nenes, A., Penner, J.E., Parther, K.A., Ramanathan, V., Ramaswamy, V., Rasch, P.J., Ravishankara, A.R., Rosenfeld, D., Stephens, G., and Wood, R.: Improving our fundamental understanding of the role of aerosol-cloud interactions in the climate system. Proc. Natl. Acad. Sci., 113, 5781-5790, https://doi.org/10.1073/pnas.1514043113, 2016.

https://doi.org/10.5194/acp-2019-519
Preprint. Discussion started: 25 July 2019


Atmospheric Chemistry and Physics Discussions

Sihto, S-L., Mikkila, J., Vanhanen, J., Ehn, M., Liao, L., Lehtipalo, K., Aalto, P.P., Duplissy, J., Petaja, T., Kerminen, V.-M., Boy, M., and Kulmala, M.: Seasonal variation of CCN concentrations and aerosol activation properties in boreal forest. Atmos. Phys. Chem., 11, 13269-13285, https://doi.org/10.5194/acp-11-13269-2011, 2011.

Stein, A.F., Draxler, R.R., Rolph, G.D., Stunder, B.J.B., Cohen, M.D., and Ngan, F.: NOAA's HYSPLIT atmospheric transport and dispersion modeling system. Bull. Amer. Meteor. Soc., 96, 2059-2077, https://doi.org/10.1175/BAMS-D-14-00110.1, 2015

Streets, D.G., Bond, T.C., Carmichael, G.R., Fernandes, S.D., Fu, Q., He, D., Klimont, Z., Nelson, S.M., Tsai, N.Y., Wang, M.Q., Woo, J.-H., and Yarber, K.F.: An inventory of gaseous and primary aerosol emissions in Asia in the year 2000. J. Geophys. Res., 108, 8809, https://doi.org/ 10.1029/2002JD003093, 2003.

Wu, Z.J., Poulain, L., Birmili, W., Größ, J., Niedermeier, N., Wang, Z.B., Herrmann, H., and Wiedensohler, A.: Some insights into the condensing vapors driving new particle growth to CCN sizes on the basis of hygroscopicity measurements. Atmos. Chem. Phys., 15, 13071-13083, https://doi.org/10.5194/acp-15-13071-2015, 2015.

Wu, Z.J., Zheng, J., Shang, D.J., Du, Z.F., Wu, Y.S., Zeng, L.M., Wiedensohler, A., and Hu, M.: Particle hygroscopicity and its link to chemical composition in the urban atmosphere of Beijing, China, during summertime. Atmos. Chem. Phys., 16, 1123-1138, https://doi.org/10.5194/acp-16-1123-2016, 2016.

Yue, D.L., Hu, M., Zhang, R.Y., Wang, Z.B., Zheng, J., Wu, Z.J., Wiedensohler, A., He, L.Y., Huang, X.F., and Zhu, T.: The roles of sulfuric acid in new particle formation and growth in the mega-city of Beijing. Atmos. Chem. Phys., 10, 4953-4960, https://doi.org/10.5194/acp-10-4953-2010, 2010.

Yue, D.L., Hu, M., Zhang, R.J., Wu, Z.J., Su, H., Wang, Z.B., Peng, J.F., He, L.Y., Huang, X.F., Gong, Y.G., and Wiedensohler, A.: Potential contribution of new particle formation to cloud condensation nuclei in Beijing. Atmos. Environ., 45, 6070-6077, https://doi.org/10.1016/j.atmosenv.2011.07.037, 2011.

Zhang, Q., Streets, D.G., Carmichael, G.R., He, K.B., Huo, H., Kannari, A., Klimont, Z., Park, I.S., Reddy, S., Fu, J.S., Chen, D., Duan, L., Lei, Y., Wang, L.T., and Yao, Z.L.: Asian emissions in 2006 for the NASA INTEX-B mission. Atmos. Chem. Phys. 9, 5131-5153, https://doi.org/10.5194/acp-9-5131-2009, 2009.

https://doi.org/10.5194/acp-2019-519
Preprint. Discussion started: 25 July 2019


Atmospheric Chemistry and Physics Discussions

**Table 1**. Statistics on the occurrence of respective air mass clusters for each month during the study period.

| Month | Cluster 1 n (%) | | Cluster 2 n (%) | | Cluster 3 n (%) | | Cluster 4 n (%) | | Cluster 5 n (%) | | Undefined n (%) | |
|---|---|---|---|---|---|---|---|---|---|---|---|---|
| *17-Apr* | *66* | *(36.7%)* | *17* | *(9.4%)* | *20* | *(11.1%)* | *43* | *(23.9%)* | *34* | *(18.9%)* | *0* | *(0.0%)* |
| *17-May* | *30* | *(16.1%)* | *12* | *(6.5%)* | *18* | *(9.7%)* | *95* | *(51.1%)* | *31* | *(16.7%)* | *0* | *(0.0%)* |
| *17-Jun* | *10* | *(5.6%)* | *0* | *(0.0%)* | *105* | *(58.3%)* | *43* | *(23.9%)* | *22* | *(12.2%)* | *0* | *(0.0%)* |
| *17-Jul* | *0* | *(0.0%)* | *0* | *(0.0%)* | *26* | *(14.0%)* | *3* | *(1.6%)* | *157* | *(84.4%)* | *0* | *(0.0%)* |
| *17-Aug* | *0* | *(0.0%)* | *4* | *(2.2%)* | *129* | *(69.4%)* | *20* | *(10.8%)* | *33* | *(17.7%)* | *0* | *(0.0%)* |
| *17-Sep* | *50* | *(27.8%)* | *12* | *(6.7%)* | *26* | *(14.4%)* | *24* | *(13.3%)* | *68* | *(37.8%)* | *0* | *(0.0%)* |
| *17-Oct* | *96* | *(51.6%)* | *31* | *(16.7%)* | *1* | *(0.5%)* | *41* | *(22.0%)* | *14* | *(7.5%)* | *3* | *(1.6%)* |
| *17-Nov* | *96* | *(53.3%)* | *42* | *(23.3%)* | *2* | *(1.1%)* | *39* | *(21.7%)* | *0* | *(0.0%)* | *1* | *(0.6%)* |
| *17-Dec* | *88* | *(47.3%)* | *84* | *(45.2%)* | *0* | *(0.0%)* | *9* | *(4.8%)* | *0* | *(0.0%)* | *5* | *(2.7%)* |
| *18-Jan* | *77* | *(41.4%)* | *77* | *(41.4%)* | *7* | *(3.8%)* | *21* | *(11.3%)* | *0* | *(0.0%)* | *4* | *(2.2%)* |
| *18-Feb* | *90* | *(53.6%)* | *50* | *(29.8%)* | *3* | *(1.8%)* | *25* | *(14.9%)* | *0* | *(0.0%)* | *0* | *(0.0%)* |
| *18-Mar* | *58* | *(31.2%)* | *38* | *(20.4%)* | *16* | *(8.6%)* | *65* | *(34.9%)* | *6* | *(3.2%)* | *3* | *(1.6%)* |
| *All data* | *661* | *(30.2%)* | *367* | *(16.8%)* | *353* | *(16.1%)* | *428* | *(19.5%)* | *365* | *(16.7%)* | *16* | *(0.7%)* |

https://doi.org/10.5194/acp-2019-519
Preprint. Discussion started: 25 July 2019


Atmospheric Chemistry and Physics Discussions

**Table 2.** Statistics for the number concentrations of cloud condensation nuclei ($N_{CCN}$) and total particles ($N_{CN}$), kappa value (κ), activation diameter (Dss) and activation ratio (AR) under four different SS conditions during the study period.

| | SS (%) | Median | 1Q | 3Q |
|---|---|---|---|---|
| $N_{CCN}$ ($cm^{-3}$) | 0.15 | 820 | 520 | 1180 |
| | 0.29 | 1220 | 720 | 1800 |
| | 0.53 | 1670 | 1010 | 2540 |
| | 0.86 | 1880 | 1140 | 2840 |
| $N_{CN}$ ($cm^{-3}$) | | 2880 | 1830 | 4690 |
| κ | 0.15 | 0.62 | 0.45 | 0.85 |
| | 0.29 | 0.41 | 0.27 | 0.57 |
| | 0.53 | 0.29 | 0.19 | 0.45 |
| | 0.86 | 0.17 | 0.11 | 0.26 |
| $D_{SS}$ (nm) | 0.15 | 101.8 | 91.4 | 113.4 |
| | 0.29 | 75.1 | 66.1 | 85.1 |
| | 0.53 | 55.2 | 48.8 | 63.8 |
| | 0.86 | 47.8 | 42.9 | 56.3 |
| AR | 0.15 | 0.261 | 0.164 | 0.380 |
| | 0.29 | 0.405 | 0.276 | 0.517 |
| | 0.53 | 0.576 | 0.430 | 0.684 |
| | 0.86 | 0.651 | 0.511 | 0.749 |

https://doi.org/10.5194/acp-2019-519
Preprint. Discussion started: 25 July 2019


Atmospheric Chemistry and Physics Discussions

**Table 3**. Statistics for the number concentration of cloud condensation nuclei ($N_{CCN}$), kappa value (κ), activation diameter ($D_{SS}$), activation ratio (AR), and concentrations of major air pollutants (i.e. CO, $NO_2$, $O_3$, and $PM_{2.5}$).

| Parameters | | | cluster 1 | | cluster 2 | | cluster 3 | | cluster 4 | | cluster 5 | |
|---|---|---|---|---|---|---|---|---|---|---|---|---|
| SS (%) | 0.15 | $N_{CCN}$ ($cm^{-3}$) | 850 | (520-1230) | 830 | (550-1080) | 820 | (480-1300) | 770 | (520-1130) | 760 | (500-1180) |
| | | Kappa | 0.69 | (0.5-0.96) | 0.69 | (0.5-0.96) | 0.56 | (0.4-0.69) | 0.56 | (0.4-0.85) | 0.56 | (0.41-0.77) |
| | | $D_{SS}$ (nm) | 98.2 | (88.2-109.4) | 98.2 | (88.2-109.4) | 107.5 | (98.2-117.6) | 105.5 | (91.4-117.6) | 105.5 | (94.7-117.6) |
| | | AR | 0.31 | (0.18-0.42) | 0.36 | (0.24-0.45) | 0.19 | (0.1-0.27) | 0.27 | (0.2-0.34) | 0.16 | (0.11-0.23) |
| | 0.29 | $N_{CCN}$ ($cm^{-3}$) | 1170 | (730-1660) | 1050 | (660-1480) | 1410 | (850-2360) | 1190 | (680-1920) | 1510 | (880-2140) |
| | | Kappa | 0.41 | (0.3-0.57) | 0.41 | (0.26-0.63) | 0.33 | (0.27-0.46) | 0.37 | (0.24-0.51) | 0.37 | (0.27-0.46) |
| | | $D_{SS}$ (nm) | 73.7 | (66.1-82) | 73.7 | (63.8-85.9) | 79.1 | (71-85.1) | 76.4 | (68.5-88.2) | 79.1 | (71-88.2) |
| | | AR | 0.43 | (0.28-0.53) | 0.46 | (0.34-0.54) | 0.34 | (0.22-0.49) | 0.42 | (0.33-0.52) | 0.29 | (0.2-0.4) |
| | 0.53 | $N_{CCN}$ ($cm^{-3}$) | 1510 | (960-2140) | 1370 | (810-1970) | 2180 | (1310-3270) | 1510 | (970-2760) | 2500 | (1600-3430) |
| | | Kappa | 0.35 | (0.23-0.45) | 0.32 | (0.21-0.45) | 0.29 | (0.21-0.36) | 0.29 | (0.17-0.4) | 0.26 | (0.17-0.36) |
| | | $D_{SS}$ (nm) | 52.4 | (47.8-59.4) | 53.3 | (47.8-61.5) | 57.3 | (52.1-61.8) | 55.4 | (49.6-66.1) | 58.4 | (54.4-67.3) |
| | | AR | 0.59 | (0.42-0.69) | 0.61 | (0.47-0.68) | 0.54 | (0.33-0.66) | 0.59 | (0.48-0.7) | 0.46 | (0.34-0.61) |
| | 0.86 | $N_{CCN}$ ($cm^{-3}$) | 1700 | (1110-2420) | 1430 | (910-2090) | 2370 | (1620-3490) | 1680 | (1090-3150) | 2740 | (1710-3900) |
| | | Kappa | 0.19 | (0.12-0.26) | 0.19 | (0.12-0.29) | 0.17 | (0.12-0.22) | 0.15 | (0.09-0.24) | 0.14 | (0.09-0.21) |
| | | $D_{SS}$ (nm) | 46.1 | (41.4-53.3) | 46.1 | (40-53.5) | 49.6 | (44.5-55.2) | 50.1 | (42.9-59.4) | 51.4 | (44.6-59.4) |
| | | AR | 0.65 | (0.5-0.74) | 0.67 | (0.53-0.75) | 0.59 | (0.47-0.72) | 0.64 | (0.56-0.75) | 0.54 | (0.43-0.68) |
| $N_{CN}$ ($cm^{-3}$) | | | 2390 | (1660-3620) | 2260 | (1400-3270) | 4660 | (3070-6710) | 2610 | (1740-4750) | 4680 | (3110-6990) |
| CO (ppb) | | | 170 | (130-240) | 160 | (120-230) | 150 | (120-200) | 170 | (120-230) | 140 | (90-210) |
| $NO_2$ (ppb) | | | 2 | (1.2-3.9) | 1.8 | (1.1-3.5) | 4.3 | (1.9-7.2) | 2.4 | (1.2-4.6) | 3.3 | (1.7-6.3) |
| $O_3$ (ppb) | | | 46 | (38-56) | 45 | (36-50) | 26 | (16-39) | 43 | (28-54) | 28 | (19-41) |
| $PM_{2.5}$ (μg $m^{-3}$) | | | 13.2 | (9.2-21.1) | 11.6 | (7.5-18.7) | 10.5 | (6.2-15.6) | 14 | (7.4-22.8) | 11 | (5.9-21) |

https://doi.org/10.5194/acp-2019-519
Preprint. Discussion started: 25 July 2019


Atmospheric Chemistry and Physics Discussions

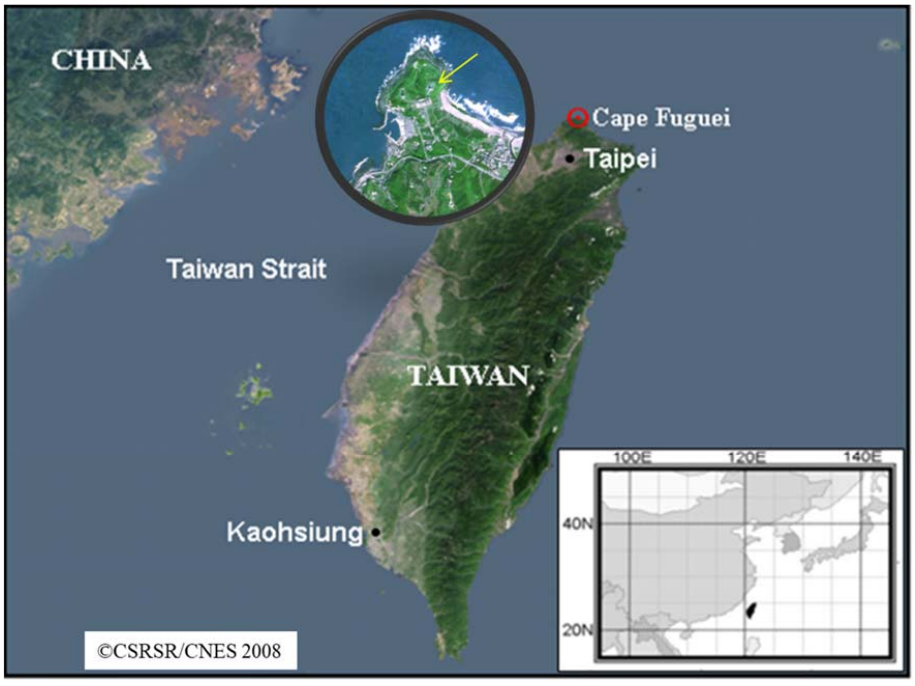


**Figure 1**. The geographical location of CAFÉ research station (25.30˚N 121.54˚E), which is exactly at the northern tip of Taiwan Island in the East Asia.

https://doi.org/10.5194/acp-2019-519
Preprint. Discussion started: 25 July 2019


Atmospheric Chemistry and Physics Discussions

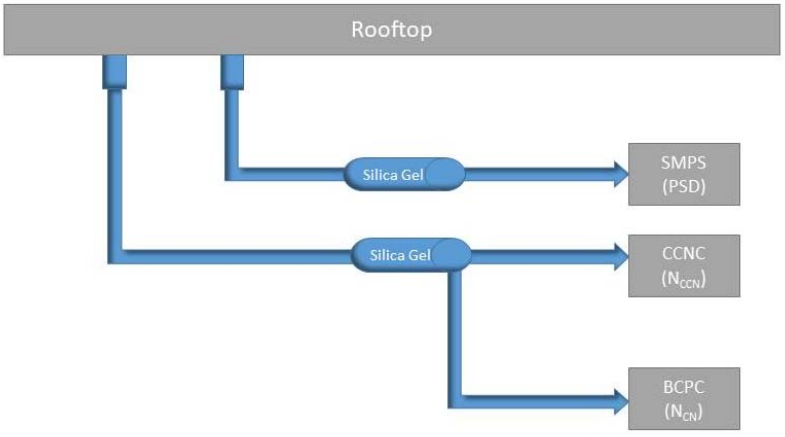


**Figure 2**. Schematic diagram for $N_{CN}$, $N_{CCN}$ and PSD measurements.

https://doi.org/10.5194/acp-2019-519
Preprint. Discussion started: 25 July 2019


Atmospheric Chemistry and Physics Discussions

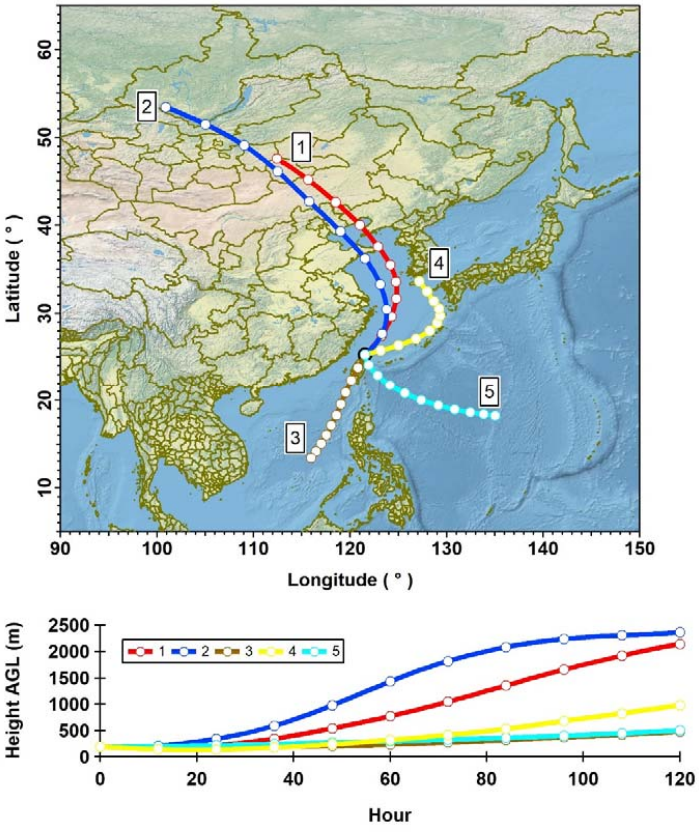


**Figure 3**. Cluster classification of 120h backward trajectories during measurement period (upper panel) and air masses heights were shown in lower panel. Air masses with both clusters 1 and 2 were originating in the inlands of the Asian Continent, but the movement of cluster 2 air masses was faster and from higher elevation. Air masses in cluster 4 were pushed by high pressure system towards the south of Korea and Japan, then moved along marine boundary slowly before reaching CAFÉ station, while Cluster 3 and 5 represent air masses originated in the South China Sea and remote Pacific region, respectively.

https://doi.org/10.5194/acp-2019-519
Preprint. Discussion started: 25 July 2019


Atmospheric Chemistry and Physics Discussions

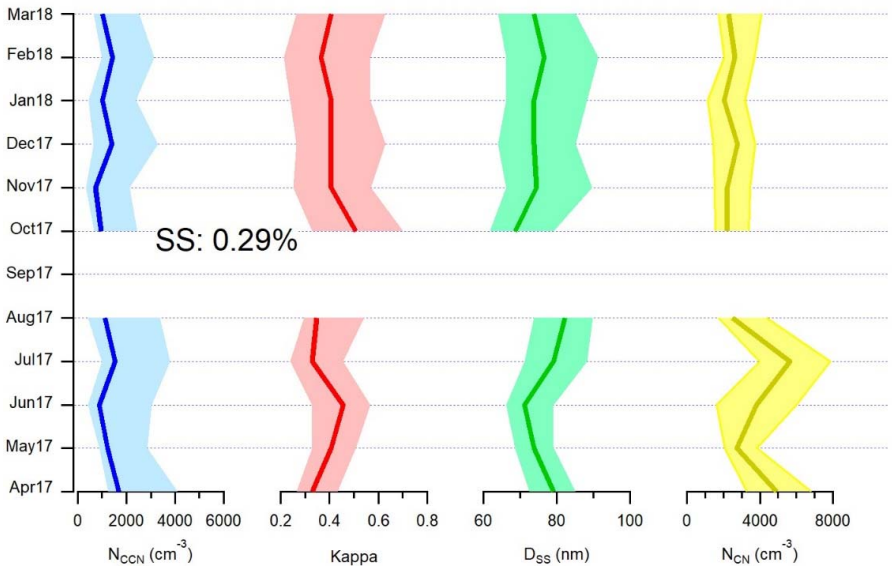


**Figure 4**. Seasonal variations in the number concentration of total particles ($N_{CN}$) and the number concentration of cloud condensation nuclei ($N_{CCN}$), kappa value (κ) and activation diameter ($D_{SS}$) measured for SS= 0.29%. Solid lines: median values, whereas shadows show upper and lower quartiles.

https://doi.org/10.5194/acp-2019-519
Preprint. Discussion started: 25 July 2019


Atmospheric Chemistry and Physics Discussions

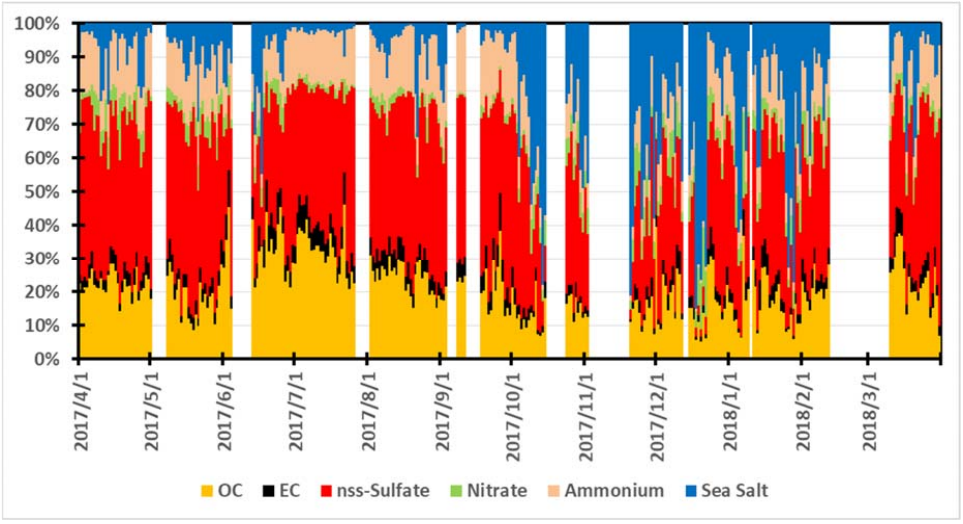


**Figure 5**. Daily mass fraction of major $PM_{2.5}$ chemical components measured during 1 April 2017 – 31 March 2018.

https://doi.org/10.5194/acp-2019-519
Preprint. Discussion started: 25 July 2019


Atmospheric Chemistry and Physics Discussions

1

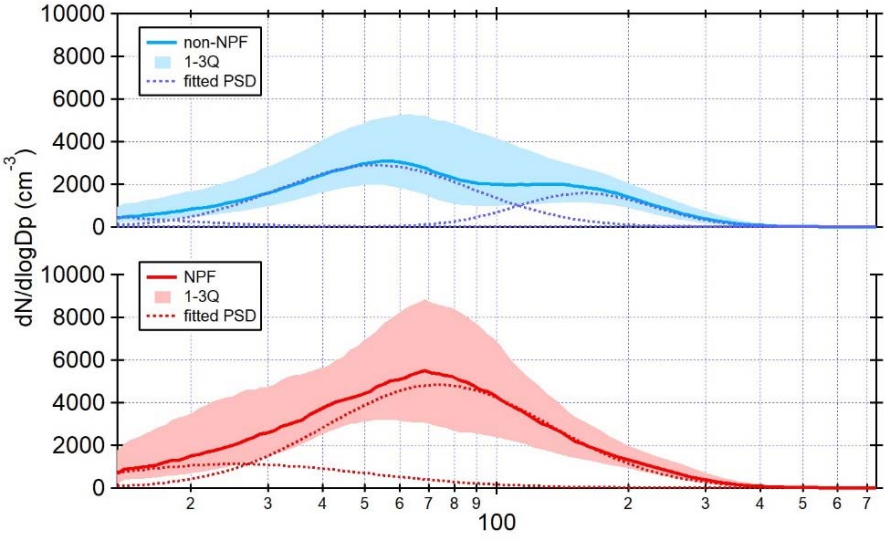


2

3 **Figure 6**. Particle size distributions observed for NPF and non-NPF events. Solid lines: median,
4 shadow: first and third quartiles, and dash lines: fitted PSD.

https://doi.org/10.5194/acp-2019-519
Preprint. Discussion started: 25 July 2019


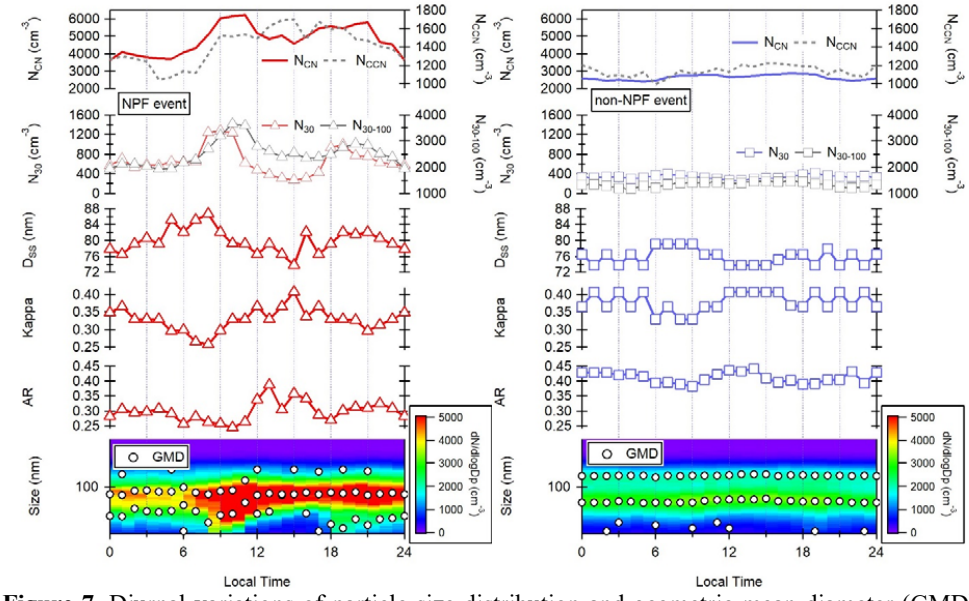


**Figure 7**. Diurnal variations of particle size distribution and geometric mean diameter (GMD), activation ratio (AR), Kappa (κ), activation diameter ($D_{SS}$), particle number concentrations of $N_{30}$, and $N_{30\text{-}100}$, and $N_{CN}$ as well as $N_{CCN}$ for NPF and non-NPF events. CCN and related parameters were measured under SS = 0.29%. GMD were calculated based on the multiple curves fitting result by DOFIT model which one to three modes were defined depends on the particle size distribution data.

https://doi.org/10.5194/acp-2019-519
Preprint. Discussion started: 25 July 2019


Atmospheric Chemistry and Physics Discussions

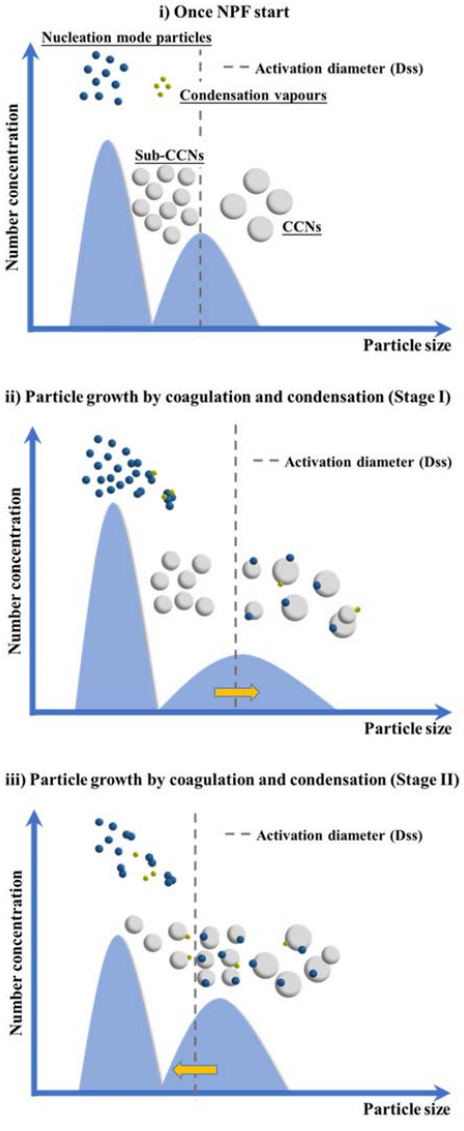


**Figure 8.** Schematic diagram of the CCN enhancement at the initial stage of NPF process: i) Nucleation mode particles formed once NPF started, ii) $D_{SS}$ increased slightly while $N_{CCN}$ increased in Stage I when existing CCN particles grew into larger size, and iii) $D_{SS}$ decreased while $N_{CCN}$ continued to increase in Stage II when sub-CCN particles grew to sufficiently large to act as CCN.